ChemComm

FEATURE ARTICLE

View Article Online
View Journal | View Issue

Cite this: *Chem. Commun.*, 2021, **57**, 302

Designing high performance conjugated materials for photovoltaic cells with the aid of intramolecular noncovalent interactions

Yahui Liu, [a] Jinsheng Song *[b] and Zhishan Bo *[ac]

Received 26th October 2020,
Accepted 29th November 2020

DOI: 10.1039/d0cc07086f

rsc.li/chemcomm

Organic semiconductors including conjugated polymers and small molecules can be applied in many fields due to their unique advantages, such as light weight, solution processability, easy functionalization *etc.* During the past ten years, we mainly focused on the design and synthesis of conjugated polymer donor materials and small molecular acceptor materials for organic solar cells and hole transport materials for perovskite solar cells. To obtain planar conjugated polymers, low cost small molecular acceptors, and dopant-free hole transport polymers, we adopted intramolecular noncovalent interactions (INCIs) as the design strategy. In this brief review, we will demonstrate that the INCI strategy is very efficient in the design of high performance photovoltaic materials.

1. Introduction

1.1 Background of 3rd generation solar cells

The development of the 3rd generation solar cells for effectively using clean, inexpensive and renewable solar energy has made significant progress in the past decade. The 3rd generation solar cells, mainly including organic solar cells[1–4] (OSCs) and perovskite solar cells,[5–8] have attracted more and more attention due to their numerous advantages, such as relatively high efficiency, easy fabrication, low cost, and light weight in comparison with their inorganic counterparts. Organic solar cells are of a sandwich structure with the active layer clamped by the transparent electrode and the back electrode. The active layer of OSCs is composed of p-type and n-type materials, which form a bulk heterojunction structure.[9–11] The p-type materials, also known as donors, could be conjugated polymers or small molecular materials that transport holes,[10,12] while the n-type

[a] *College of Textiles & Clothing, Qingdao University, Qingdao 266071, China*
[b] *Engineering Research Center for Nanomaterials, Henan University, Kaifeng 475004, China. E-mail: songjs@henu.edu.cn*
[c] *Key Laboratory of Energy Conversion and Storage Materials, College of Chemistry, Beijing Normal University, Beijing 100875, China. E-mail: zsbo@bnu.edu.cn*

Yahui Liu

Yahui Liu received his BS degree in Beijing Normal University at 2013. He joined Prof. Zhishan Bo's group for his doctoral research and received his PhD degree at Beijing Normal University in 2018. Then, he worked as a research assistant in Prof Bo's group. In 2020, he joined Qingdao University and his research interest is the design, synthesis and application of functional materials such as conjugated polymers, fused ring electron acceptors, and fullerene derivatives.

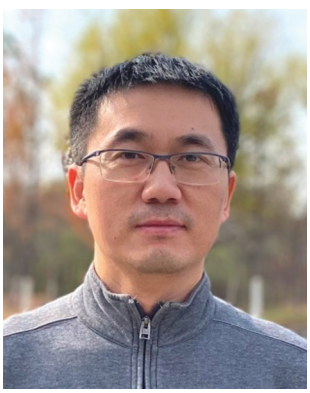

Jinsheng Song

Jinsheng Song received his bachelor and master degrees from Hunan University (2000–2007). He joined Prof. Zhishan Bo's group in 2007 and received his PhD degree from the Institute of Chemistry, Chinese Academy of Sciences (ICCAS) in 2010. Then he worked with Prof. Larry Dalton as a research associate at the University of Washington (UW) (2010–2012). In 2012, he joined Henan University and he is currently appointed as a full professor. The main research interests are conjugated materials designs and applications in organic solar cells, electro-optics, bio-imaging etc.

materials, so-called acceptors, could be fullerene derivatives, small molecular electron acceptors or conjugated polymers that transport electrons.[13,14] Before 2015, considerable efforts had been devoted to the exploration of novel p-type conjugated polymers and the use of them as donor materials to fabricate OSCs with fullerene derivatives as the acceptor materials.[12,15–19] In the last five years, the main research interest of the organic photovoltaic field has moved to the nonfullerene acceptors.[20,21] Significant improvements in the power conversion efficiency (PCE) of OSCs have been recently achieved and a PCE up to 17% has been reported.[4,22–25] The development of novel π-conjugated structures and device engineering technologies has played a pivotal role in the device performance improvement.[26–28]

As an important component of the active layer in organic solar cells, various conjugated polymers have been designed and synthesized.[2,12,29,30] High performance organic solar cells require that the conjugated polymers should have intensive absorption and appropriate energy levels. Besides the above prerequisite, high performance organic solar cells also require that the conjugated polymer should have good processability and the polymer chains should be able to form closely packed structures to facilitate hole transport.[12,18,31] As for high performance small molecular acceptors, they usually possess multi-fused ring structures.[32–35] The synthesis of such fused ring acceptors is usually tedious and highly expensive. Besides, perovskite solar cells based on the commonly used hole transport materials such as spiro-OMeTED usually exhibit poor stability and durability.[36,37] To solve the above mentioned problems, we utilized intramolecular noncovalent interactions (INCIs) as a design strategy in the synthesis of conjugated polymers and small molecular acceptors.[38,39] As expected, all of these newly designed materials exhibited excellent device performance (*vide infra*).

1.2 Noncovalent interactions

Interaction between permanent multipoles, between a permanent multipole and an induced multipole, and between an instantaneous time variable multipole and an induced multipole can be considered as noncovalent interactions.[40,41] The noncovalent interaction is an interesting research topic in the field of chemistry (supramolecular chemistry, theoretical chemistry, *etc.*) and a powerful tool for material science.[42] The concept of noncovalent interaction can be traced back to the 19th century. van der Waals first put forward this concept during the modification of state equation.[43] Further investigation demonstrates that the noncovalent interaction contains abundant content, such as hydrogen bonds, ionic bonds, halogen bonds, chalcogen bonds, agostic bonds, *etc.*[44,45] Yang *et al.* developed a visualized approach to map or analyze noncovalent interaction according to electron density and its reduced gradient.[46,47] There are many classification methods or names of noncovalent interactions. For example, they are collectively named secondary bonding or secondary valence forces by some researchers. This definition was initially used to describe the intermolecular interactions with length less than the sum of van der Waals radii.[48,49] Besides, some researchers divide noncovalent interaction into σ- and π-hole bonds according to surface electrostatic potential holes.[50,51]

Generally speaking, the noncovalent interactions can be roughly divided into intermolecular and intramolecular noncovalent interactions.[52] Accordingly, supramolecular chemistry mainly focuses on the intermolecular interaction, which covers the structures and functions of the entities formed by two or more chemical species.[53] Moreover, intermolecular interactions such as hydrogen bonds, van der Waals forces, *etc.*, which widely exist in chemical and biological systems, can be used to construct functional materials, drug molecules, and biological materials. Unlike intermolecular interactions, the INCIs can only be found in specific materials. Sometimes, the inter- and intra-molecular noncovalent interactions can coexist. Herein, we mainly focus on the INCIs. Currently, there are usually two methods to verify the existence of INCIs. Single crystal structure characterization provides direct proof and density functional theory (DFT) calculation offers reliable predictions. If INCIs are formed, the distance of the corresponding two atoms will be larger than the covalent radii, but significantly smaller than the sum of van der Waals radii.

1.3 Materials based on intramolecular noncovalent interactions

Noncovalent interactions are widely used in many fields including catalysis, biological medicine, organic semiconduction, *etc.*[53,54] For example, supramolecular polymers, which originated from the integration of polymer science and supramolecular chemistry, could comprise many kinds of intermolecular interactions (H-bonding, metal-coordination bonds, host–guest interactions *etc.*).[55] In comparison to the conventional covalent bonded polymers, such noncovalent interactions would render the materials with lower binding energy, reversible formation and dissociation,[56] dynamic reorganization, good processability, self-healing[57] and stimuli responsiveness.[58] Besides intermolecular noncovalent interactions, INCIs also possess the same essence, which could regulate the molecular configuration. So, what would happen if we brought it into the material construction, especially

Zhishan Bo

Zhishan Bo received his bachelor, master, and doctor degrees from Jilin University in 1989, 1994, and 1997, respectively. From 1997–2002, he did his postdoctoral research at Free University Berlin and North Carolina State University. In 2002, he was appointed as a full professor at the Institute of Chemistry, Chinese Academy of Sciences (ICCAS). In 2010, he joined Beijing Normal University and his research interests focus on conjugated functional materials: design, synthesis and applications.

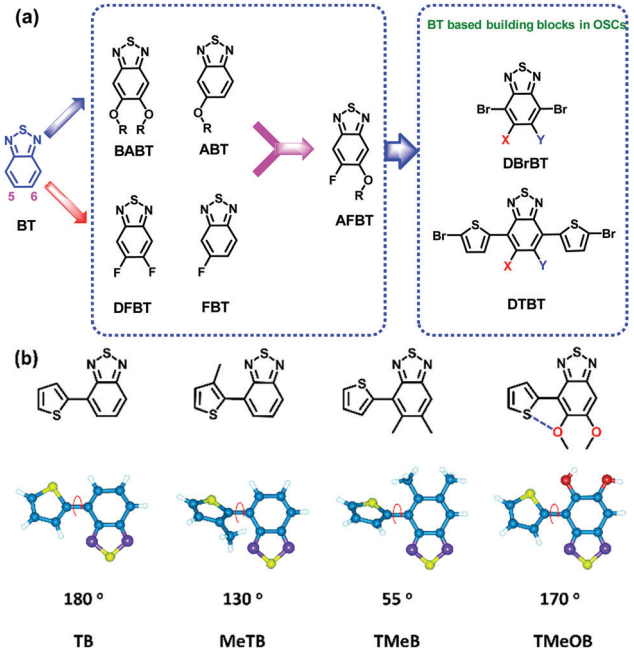

Fig. 1 (a) Evolution of the BT units, and (b) dihedral angles of TB, MeTB, TMeTB and TMeOB according to DFT calculations.[71]

the conjugated materials? Previously, Mugesh and coworkers prepared various ebselen analogues and correlated their catalytic activities with the Se···O intramolecular interactions.[59,60] Goldstein and Burling showed that the conformations of thiazole and selenazole nucleosides can be stabilized by the intramolecular electrostatic interaction of S···O and Se···O.[61] To verify the impact of INCIs on the properties of conjugated polymers, we employed alkyloxy substituted dibenzothiophene as the donor unit and benzothiadiazole as the acceptor unit to construct D–A alternating copolymers and demonstrated that the intramolecular S···O interaction can generate planar polymer backbones with stronger intramolecular charge transfer (ICT) effect and red-shifted absorption.[62] Almost at the same time, Huang *et al.* utilized the intramolecular S···O interactions, namely, "conformational locks" to fabricate high-mobility polymer semiconductors with a planar backbone.[63]

During the last ten years, we have been devoted to exploring novel conjugated materials including alternating copolymers and small molecules, where we put forward an idea to construct planar molecular skeletons *via* the assistance of INCIs. The concept has been first applied to the design and synthesis of D–A alternating conjugated polymers with 3,4-bis(alkyloxy)benzothiadiazole as the electron deficient unit. As shown in Fig. 1a, the intramolecular S···O and N···H interactions could generate a planar conformation for the thiophene-3,4-bis(alkyloxy)benzothiadiazole-thiophene (Th-BABT-Th) unit.[64] With this concept, a variety of conjugated polymer donors with planar molecular backbones were developed.[62,65,66] Later, further enhancing the performance of OSCs based on fullerene derivatives has encountered a bottleneck, and then research interest in this field has switched to the nonfullerene acceptors.[67,68] We first applied the concept of INCIs in the design and synthesis of nonfullerene acceptors.[69] Unexpectedly, the

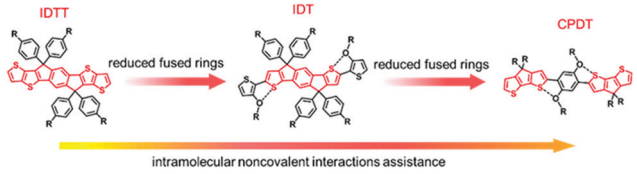

Fig. 2 Typical chemical structures of the fused ring core and nonfused ring core.

photovoltaic devices based on such acceptor molecules could achieve high PCEs and low energy losses.[70] Most importantly, such noncovalent auxiliary strategy can partially or completely replace the covalent bonds, and thus reduce the synthetic expense as shown in Fig. 2. Additionally, we also use such an INCI strategy in the design and synthesis of ladder-like conjugated polymers, which could be used as dopant-free hole transport materials for perovskite solar cells.[38] In this review, we briefly summarized the material evolution by virtue of such an INCI strategy.

2. Noncovalent interaction assisted conjugated polymers for organic solar cells

2.1 Planar conjugated polymers with intramolecular noncovalent interaction

High performance organic solar cells require that the active layer possesses a bulk heterojunction structure, namely, the donor polymer and the acceptor molecule form a nanoscale phase separation with a bicontinuous network.[72,73] Additionally, the blend film should have high and balanced charge mobilities. To achieve this goal, conjugated polymer chains should be able to form closely packed structures in the film on the one hand.[18] On the other hand, the conjugated polymers should also have good solubility in the processing solvent.[17] However, good solubility and close packing are usually contradictive. To solve this dilemma, we first designed and synthesized conjugated polymers with a planar backbone with the aid of INCIs.

The polymers (HXS-1) are composed of a linear alkyl chain substituted 2,7-linked carbazole donor unit, thiophene π-bridge unit, and 5,6-bis(alkyloxy) substituted benzothiadiazole (BABT) acceptor unit.[64] The INCIs of S···O and N···H would ensure the Th-BABT-Th block with a coplanar configuration as shown in Fig. 1. In the meantime, the two alkyloxy side chains in the BT unit would further improve the solubility of the target polymers since the intramolecular noncovalent interaction existed in the film state may dynamically be broken in the solution state. As expected, HXS-1 exhibits a relatively planar polymer backbone, good solubility in 1,2-dichlorobenzene, and close packing in the solid state. The HXS-1:$PC_{71}BM$ blend film exhibits high and balanced electron/hole mobilities. Devices based on HXS-1:$PC_{71}BM$ demonstrate a PCE of ~5.4%, which is also one of the best results at that time. Subsequently, the Th-BABT-Th unit has also been utilized for the construction of some other polymers.[74] For example, the Th-BABT-Th unit was also

used to combine with the 9,9-dialkyl-9*H*-dibenzosilole donor unit to construct conjugated polymers (PSiF-1a and PSiF-1b).[75] The dioctyl substituted PSiF-1b exhibits good solubility in the commonly used organic solvent, and thus high molecular weight polymers (M_n: 102 kg mol^{-1}) can be achieved. Consequently, a PCE of 6.05% was achieved for devices based on PSiF-1b:$PC_{71}BM$.

Except for the BABT, some other BT derivatives (FBT, DFBT, AFBT *etc.*) and the evolutive building blocks (DBrBT, DTBT *etc.*) are used in OSCs as shown in Fig. 1a, which could form planar conjugated polymer skeletons *via* INCIs (F···S, O···S or F···H). For example, the introduction of the planar Th-DFBT-Th unit could also lower the HOMO energy level and generate a high V_{oc} for the devices. Meanwhile, the strong noncovalent interaction that originated from the F atom would greatly reduce the solubility and processability of the final polymers as observed for PSiF-DTDFBT, leading to poor photovoltaic performance.[76] To well balance these issues, a combination of fluorine and alkyloxy is designed in AFBT. Based on this unit, a similar polymer PSiF-2 could achieve a significantly improved PCE of 6.41% when blended with $PC_{71}BM$.[77] Through copolymerization with the dibenzopyran unit, the photovoltaic performance of PDBPTBT-4 based devices could be further enhanced to 7.06%.[78]

9,9-Dialkylfluorene, which has a sp^3-hybridized carbon at the 9-position, is one of the popular electron donating blocks used for the synthesis of light-emitting and photovoltaic materials.[79–82] However, the two alkyl chains at the 9-position of the fluorene unit will prevent the polymer chains from forming close π–π stacking in the solid state. To further increase the planarity of the polymer backbone, we used 9-alkylidene-9*H*-fluorene instead of 9,9-dialkylfluorene as the donor unit, BABT as the acceptor unit, and thiophene as the π bridge to construct planar conjugated polymers PIF-1 as shown in Fig. 3.[83] Finally, PIF-1:$PC_{71}BM$ based PSCs exhibit a PCE of 6.2%, which is almost two times higher than that of devices based on PFTBTT as shown in Fig. 3. Later, the planar conjugated polymer PIF-2, which contains the diphenyl substituted 9-alkylidene-9*H*-fluorene unit and BABT unit, was synthesized. A further increased PCE of 6.52% was achieved for the PIF-2 based devices.[66]

BABT was also used to construct conjugated polymers (PBDTAF-1, PBDTAF-2 and PBDTAF-3) by alternating with the benzodithiophene (BDT) unit.[84] These polymers possess planar backbones, display great impact on the morphology of blend films and present reasonable photovoltaic performance with a PCE of 6.88% when using $PC_{71}BM$ as the acceptor. After the side

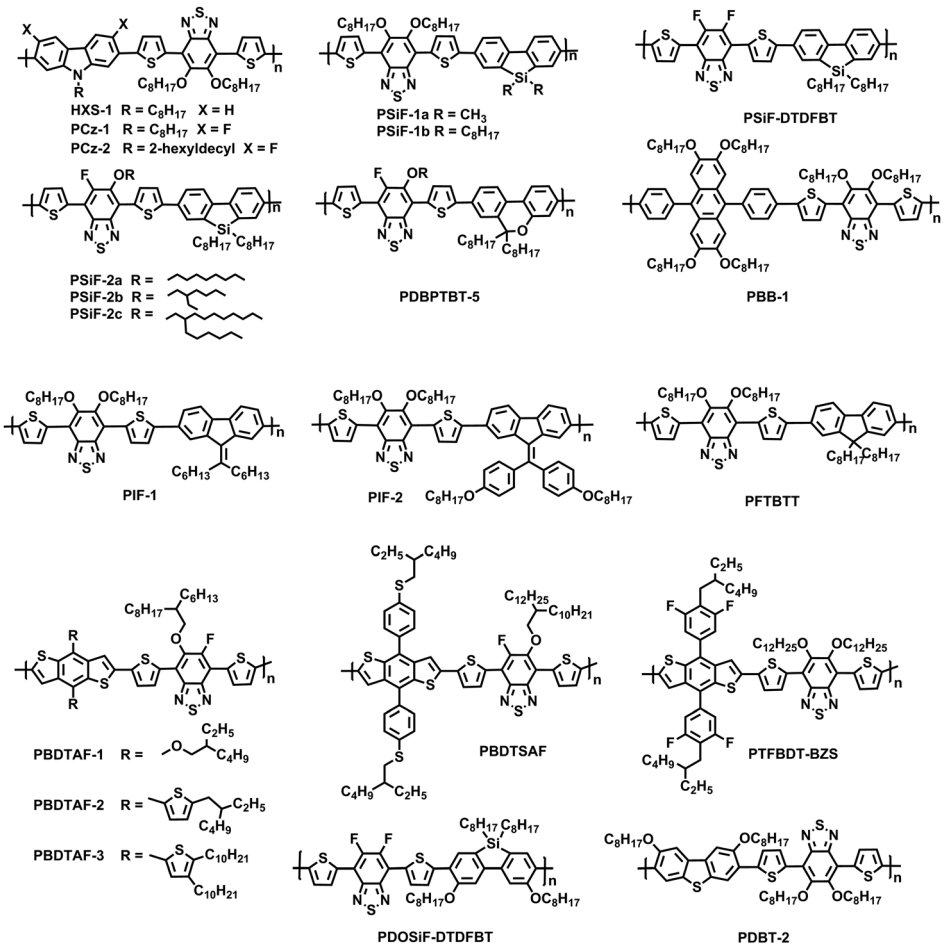

Fig. 3 Chemical structures of polymer donors with BT derivatives as the acceptor units.

chains are replaced by alkylphenyl ones, an even higher PCE of 7.7% is achieved for the PBDTSAF:$PC_{71}BM$ based devices, which also displayed a good tolerance to the variation of film thickness.[85] Such thickness insensitive characteristics are closely related to its significantly improved SCLC hole mobility ($\mu = 6.0 \times 10^{-2}$ cm^2 V^{-1} S^{-1}) that should be ascribed to its planar conjugated backbones and close molecular packing. Polymer PTFBDT-BZS with 4-alkyl-3,5-difluorophenyl as the side chain at the BDT unit displays a closed π–π stacking distance of 3.69 Å. As anticipated, this polymer displays a low HOMO energy level and a high PCE of 8.24% for the as-cast devices when blended with $PC_{71}BM$.[65] This polymer also presents a good compatibility with nonfullerene acceptors (*e.g.* IDIC), and a high PCE of 11.03% is achieved.[86] The charge generation and recombination dynamic studies suggest the existence of extremely efficient charge generation channels in the blend system, which is associated with the more ordered face-on molecular orientation, appropriate domain size and rather pure domain. In all, the above examples demonstrate that intramolecular noncovalent interaction is very useful for the construction of high efficiency planar donor polymers.

2.2 Multiple noncovalent interaction assisted strategy for planar conjugated polymers

Generally, conjugated polymers possess a single-stranded polymer main chain; the donor, spacer and acceptor units can usually freely rotate around the C–C single bond; and thus the planarity of the polymer chain will be interfered with. Conjugated polymers comprising multiple noncovalent S···O, O···H, F···S or F···H interactions between donor and acceptor units can produce a planar ladder-like polymer structure as shown in Fig. 3. As expected, ladder-like PDOSiFDTDFBT displays a high field effect transistor (FET) hole mobility up to 3.3×10^{-2} cm^2 V^{-1} S^{-1}, which is much higher than the counterpart without intramolecular noncovalent interactions. A similar phenomenon is also observed for the dibenzothiophene based polymers.

PCz-1 comprising F···S and F···H interactions between the donor and acceptor units exhibits a poor solubility in commonly used organic solvents, thus only low molecular weight (M_n = 9.1 kg mol^{-1}) materials could be prepared.[87] Replacing the octyl chain at the 9-position of the 3,6-difluorocarbazole unit with a branched 2-hexyldecyl chain could increase the solubility of the resulting polymers without interfering with the main chain conformation. With an improved processability, PCz-2 gives an elevated PCE of 7.39%, which shows 37% improvement in comparison to HXS-1.[88]

In the meantime, organic–inorganic halide perovskite solar cells have received wide-spread attention due to their outstanding performances.[89] The hole transport layer plays a very important role in fabricating high performance devices, in which spiro-OMeTED is a widely used hole transport layer material. High power conversion efficiency up over 22% has already been achieved for devices with spiro-OMeTED as the hole transport layer,[90] however, stability is still a big issue encountered for such types of devices.[91–93] Devices with Li-TFSI doped spiro-OMeTED as the hole transport layer usually exhibit very poor long-term stability. To enhance the long-term stability of perovskite solar cells, varied

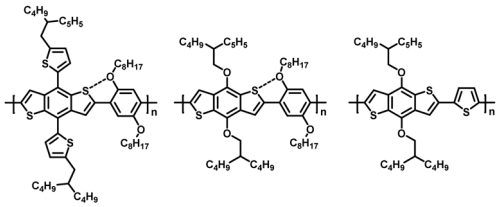

Fig. 4 Chemical structures of P1, P2 and P3.

hole transport materials including conjugated polymers and small molecules have been used. Recently, we have designed and synthesized a series of ladder-like conjugated polymers and used them as hole transport layers for perovskite solar cells.[38] The intramolecular noncovalent S···O interaction can endow such ladder-like conjugated polymers with a planar polymer backbone, which favors the polymer to pile closely and achieve high hole mobility for the polymer films. Through modulating the two monomers, conjugated polymers P1, P2 and P3, shown in Fig. 4, can be precisely designed with controllable energy levels, high hole transport mobilities, *etc.* Among them, ladder-like conjugated polymer P1 demonstrates the highest hole mobility and matched energy levels with perovskite active layers. Hence, an excellent PCE of 18.30% is achieved with P1 as the HTM. Subsequently, the modified ladder-like conjugated polymer P-Si,[39] shown in Fig. 5, can also be used as a hole transport medium between the perovskite and spiro-OMeTAD layer and the resulting devices exhibit better long-term stability in an ambient environment.

3. Noncovalent interaction assisted FREAs for organic solar cells

Because of the limitations such as weak absorption, fixed energy level, difficulty of purification *etc.* for the fullerene based acceptors, nonfullerene acceptors have been rapidly developed during the past several years. In 2015, Zhan *et al.* first reported a novel FREA ITIC,[94] which can give a comparative photovoltaic performance with fullerene acceptors. Subsequently, numerous FREAs have been designed and synthesized. Some typical FREAs are shown in Fig. 5.[86,94–98] The typical A–D–A type FREAs are normally composed of three parts: ladder-type fused core, bulky side chains and electron-withdrawing terminal groups. The ladder-type fused ring structure can endow the molecular backbone with a planar conformation, and thus better delocalization of the π-electrons can be achieved. The bulky side chains can improve the solubility of the acceptor molecules and prevent them from forming large aggregates. The charge transfer effect from the donor core to the terminal acceptor

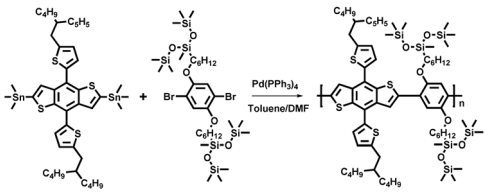

Fig. 5 Synthetic route to P-Si, reagents and conditions.

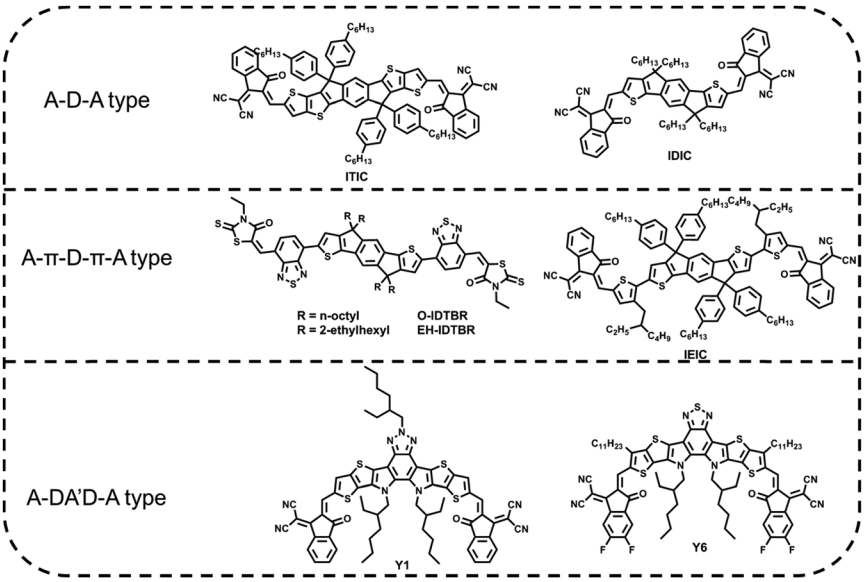

Fig. 6 Typical chemical structures of FREAs.

unit can bring about a broad absorption for the acceptor molecules.[68] The close π–π stacking of terminal groups can ensure that the acceptor molecules can form a transport path for electrons. With the evolution of A–D–A type acceptors, the derived A–π–D–π–A and A–DA′D-A type molecules also attract a lot of attention. Currently, the PCEs of OSCs based on FREAs have approached 18%, demonstrating great application potential.[22,23,99]

However, the synthesis of FREAs will inevitably increase the synthetic expense due to the multi-step synthesis of fused ring cores as shown in Fig. 6, where complicated ring closure reactions are necessary.[100] For simplifying the synthesis, we have suggested the use of noncovalently fused ring acceptors instead of FREAs. We adopted the intramolecular noncovalent interactions to replace the chemical bonds to construct the planar ladder-like core. Noncovalently fused ring electron acceptors (NC-FREAs), which are actually non-fused ring structures, can be synthesized by using a modular strategy. Therefore, the synthesis cost for such acceptors could be much cheaper than the corresponding FREAs (Fig. 7). Herein, we will mainly divide NC-FREAs into two categories according to the central donor units and the details are as follows.

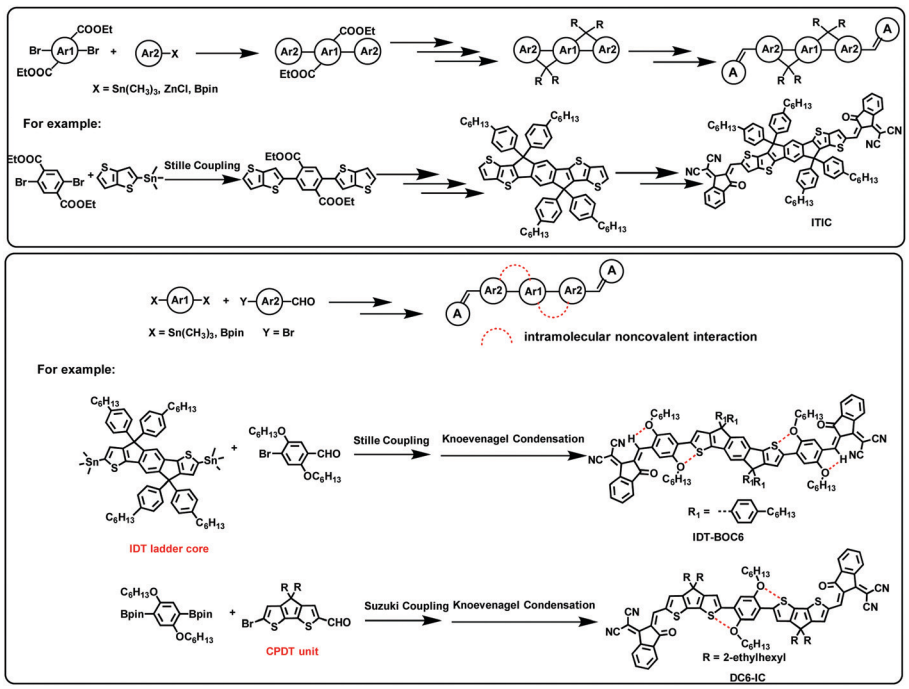

Fig. 7 The synthetic routes of FREAs and ladder-like NFAs.

3.1 Nonfused NFAs with IDT as the core unit

In 2017, we first reported two NC-FREAs (IDT-BOC6 and IDT-BC6), in which dihexylbenzene and bis(hexyloxy)benzene are used as the bridge units.[69] As shown in Fig. 8, the simplified IDT-BOC6 can form S···O and H···O INCIs to force the molecular backbone to adopt a flat conformation, which is similar to the nine membered fused ring core. In comparison, IDT-BC6 without INCIs tends to form a twisted molecular skeleton. In addition, IDT-BOC6 exhibits broader absorption, higher electron mobility, and higher photoluminescence quantum yield. The intuitive image of the blend films based on IDT-BOC6 and IDT-BC6 is also shown in Fig. 9. The polymer donor PBDB-T can preferentially separate out to form nanofibril networks, and then the small molecular acceptors precipitate within the polymer fibril networks, and finally the blend films form nanoscale bicontinuous networks. As for IDT-BOC6 based blend films, the acceptors display favorable planarity due to the existence of S···O and H···O INCIs and can form close π–π stacking, whereas IDT-BC6 acceptors tend to form disordered molecular accumulation due to the twisted molecular geometries. PSCs based on IDT-BOC6 furnished a power conversion efficiency (PCE) of 9.6%. In contrast, PSCs based on similar acceptor IDT-BC6 without INCIs only gave a PCE of 2.3%. Most importantly, the synthesis of NC-NFEAs could significantly reduce the synthetic expense and reach the same goal as FREAs.

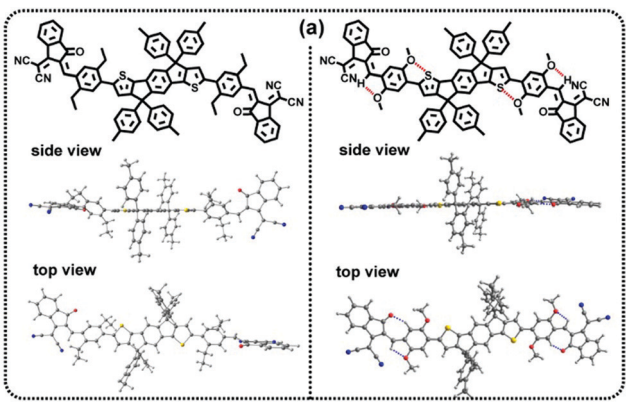

Fig. 8 Simulated molecular geometries obtained by DFT calculations for simplified molecules of IDT-BC6 (left) and IDT-BOC6 (right). Copyright 2017, American Chemical Society.

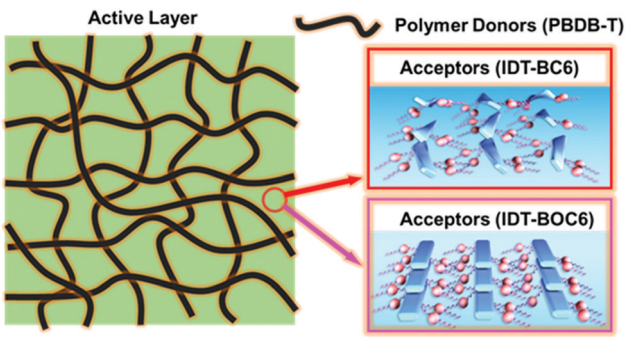

Fig. 9 Intuitive film morphology of PBDB-T:IDT-BOC6 and PBDB-T:IDT-BC6 blend films.

Subsequently, the π-bridge was replaced by 3,4-bis(alkyloxy)thiophene and three novel NC-FREAs (ITOIC, ITOIC-F and ITOIC-2F) with different fluorinated electron-withdrawing groups are designed and synthesized.[101] Such molecular design would not only provide a planar molecular backbone, but also produce a hierarchical supramolecular self-assembly through the terminal group stacking. More specifically, the INCIs (S···O and O···H) could induce and stabilize the planar conformation of the molecular backbone and the intermolecular electrostatic interaction by terminal groups could reinforce the π–π stacking (as shown in Fig. 10). In addition, the introduction of fluorine atoms would also help to enhance the interaction of terminal groups. Finally, based on this precise molecular design strategy, ITOIC, ITOIC-F and ITOIC-2F based devices achieve PCEs of 8.87%, 10.65% and 12.17%, respectively. Besides, the chlorinated one ITOIC-2Cl could give a PCE of 9.37% after blending with PBDB-T, and the blend film formed a bicontinuous interconnected network and displayed a high charge transport mobility.

As is well-known, the position of the alkyloxy side chains would directly influence the molecular conformation as well as the electronic characteristics of the acceptor molecules. In 2018, Liu *et al.* and our group simultaneously reported a novel acceptor IDTOT2F, which bears two alkoxyl chains on the central indacenodithiophene (IDT) unit to lock the planar conformation of the backbone with S···O INCIs, and the control molecule without alkyloxy side chains is denoted as IDTT2F.[102,103] Such molecular design would bring two merits: first, the introduction of two alkyloxy side chains onto the central IDT unit could guarantee good solubility and processability; second, the S···O INCIs would stabilize the planar conformation of the molecular skeleton and result in an ordered packing as confirmed by the GIWAXS results shown in Fig. 11. These special characteristics of IDTOT2F are beneficial to improving the miscibility with the polymer donor and forming the preferred interpenetrating binary networks with favored molecular orientation in the blend films. Hence, an excellent PCE of 12.79% is achieved with IDTOT2F-based devices, which is much higher than that of the IDTT2F-based control devices (8.85%).

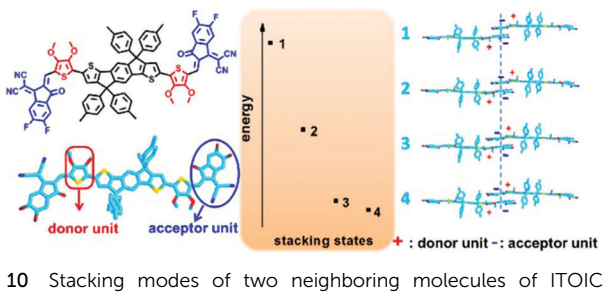

Fig. 10 Stacking modes of two neighboring molecules of ITOIC-2F determined *via* DFT calculation. Copyright 2018, American Chemical Society.

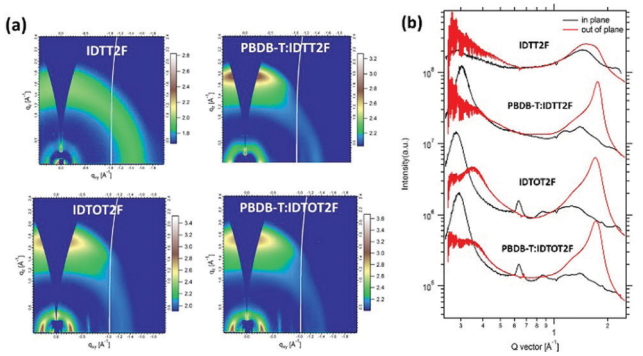

Fig. 11 (a) GIWAXS 2D patterns of IDTT2F, IDTOT2F, PBDB-T:IDTT2F, and PBDB-T:IDTOT2F films. (b) Corresponding scattering profiles in the IP (black) and OOP (red) directions. Copyright 2018, American Chemical Society.

Lately, a series of A–π–D–π–A type nonfullerene acceptors (NFAs) IDTCN-C, IDTCN-O and IDTCN-S have been designed and synthesized, which bear alkyl, alkyloxy and alkylthio side chains at the outer position of the π bridge unit, respectively.[104] The introduction of a side chain at the outer position of the π bridge unit can endow the terminal moiety with a confined planar conformation due to the steric hindrance effect. These acceptors tend to form close π–π stacking with the favorable face-on orientation. Due to the slightly up-shifted LUMO level and more balanced charge transport, a PCE of 13.28% is obtained for the IDTCN-O based as-cast devices. These research studies demonstrate that the local planarity of the terminal group is as important as the planarity of the whole molecule and the side chain engineering is an effective way to tune the molecular conformation (Table 1).

Table 1 Photovoltaic parameters of A–π–D–π–A type NFAs with IDT as the core unit

NFAs	HOMO (eV)	LUMO (eV)	E_g (eV)	V_{oc} (V)	J_{sc} (mA cm^{-2})	FF	PCE (%)	Ref.
IDT-BOC6	−5.51	−3.78	1.63	1.01	17.52	0.54	9.60	69
IDT-BC6	−5.55	−3.82	1.75	0.92	5.63	0.44	2.30	69
ITOIC	−5.48	−3.75	1.55	1.02	15.73	0.55	8.87	101
ITOIC-F	−5.52	−3.82	1.50	0.95	18.60	0.61	10.65	101
ITOIC-2F	−5.57	−3.87	1.45	0.90	21.04	0.65	12.17	101
IEICO	−5.32	−3.95	1.34	0.82	17.70	0.58	8.40	109
IEICO-4F	−5.44	−4.19	1.24	0.74	22.80	0.59	10.00	110
IEICO-4Cl	−5.56	−4.23	1.23	0.73	22.80	0.62	10.30	111
IDTOT2F	−5.54	−3.94	1.44	0.85	20.87	0.72	12.79	102
IDTO-T-4F	−5.49	−3.88	1.45	0.86	20.12	0.73	12.62	103
IDT-Tz	−5.62	−4.09	1.53	0.88	13.67	0.71	8.52	108
IDT-EDOT	−5.43	−3.80	1.63	0.86	21.34	0.62	11.32	105
IDT-PDOT	−5.39	−3.77	1.62	0.85	5.26	0.49	2.18	105
IDTO-Se-4F	−5.48	−3.90	1.40	0.83	18.55	0.69	10.67	103
IDTO-TT-4F	−5.39	−3.89	1.38	0.86	17.21	0.69	10.21	103
IDT-3MT	−5.68	−4.16	1.52	0.95	14.43	0.61	8.40	112
ORCN	−5.37	−3.56	1.64	0.87	11.50	0.62	6.40	113

Besides, the electron rich 3,4-ethylenedioxythiophene and 3,4-propylenedioxythiophene are selected as the π bridge units to construct IDT-EDOT and IDT-PDOT, respectively.[105] Interestingly, these two acceptors display significantly different PCEs. A much higher PCE of 11.32% is achieved with IDT-EDOT as the acceptor, whereas the photovoltaic devices based on IDT-PDOT only give a PCE of 2.18%. Further investigations demonstrate that the lower molar absorption coefficient, larger π–π stacking distance and inferior charge transport mobility can well explain the poor photovoltaic performance of IDT-PDOT based devices. Subsequently, IDT-PDOT-C6 with 3,4-propylenedioxythiophene bearing two hexyl side chains as the π bridge unit is synthesized. IDT-PDOT-C6 is introduced to the PBDB-T:IDTT-OB binary system as the third component to fabricate ternary OSCs, where IDTT-OB is an asymmetric acceptor developed by our group. The ternary devices display an elevated PCE of 13.04%, which is much higher than the two corresponding binary devices. The V_{oc}, J_{sc} and FF are simultaneously enhanced and a low E_{loss} is achieved for the ternary devices.[106] When $PC_{71}BM$ is introduced to the PBDB-T:IDT-EDOT system as the third component, the ternary devices realize photovoltaic performance enhancement, and the device performance is not sensitive to the ratios of the two acceptors. Interestingly, the ternary devices display enhanced phase purity and increased EQE_{EL}.[107]

In short, the π bridge in A–π–D–π–A type acceptors, which acts as the crucial linker between the donor core and the electron deficient terminal group, can tune the molecular conformation, extend the effective conjugation length, adjust the energy levels, and regulate the morphology of the blend films.[108–113] Until now, varied π bridge units and central IDT derivatives are used to construct the A–π–D–π–A type nonfullerene acceptors with the aid of noncovalent interactions as shown in Fig. 12.

3.2 Nonfused NFAs based on the cyclopentadithiophene (CPDT) unit

A fused ring donor unit plus two flanked π-bridges could be a simple strategy to extend the conjugation length of NFAs. Alternatively, the connection of two fused ring donor units by a central π-bridge unit can also be used to accomplish such function. CPDT is a commonly used electron donor unit, which can be adopted to construct low bandgap and high mobility conjugated materials. In 2018, Chen *et al.* reported a nonfused NFA called DF-PCIC with two CPDT units. For DF-PCIC, the F···H INCIs can help to generate nearly planar molecular geometry. After device optimization, a high PCE of 10.14% is achieved with a high FF of 0.72.[114] Besides, devices based on these acceptors display a good thermal stability as 70% of the original PCE could be still preserved after thermal treatment at 180 °C for 12 h. Subsequently, different fluorinated benzene cores such as 2,3,5,6-tetrafluorobenzene and 2,5-difuoro-3,6-dimethoxybenzene were used to synthesize nonfused NFAs, which could tune the molecular packing, the domain size and charge transport mobility *etc.* (Fig. 13).

In the meantime, we construct a series of low-cost NFAs (DOC6-IC, DOC8-IC, DOC2C6-IC, and DOC2C6-2F) with a ladder-like core with the aid of S···O INCIs to avoid the tedious

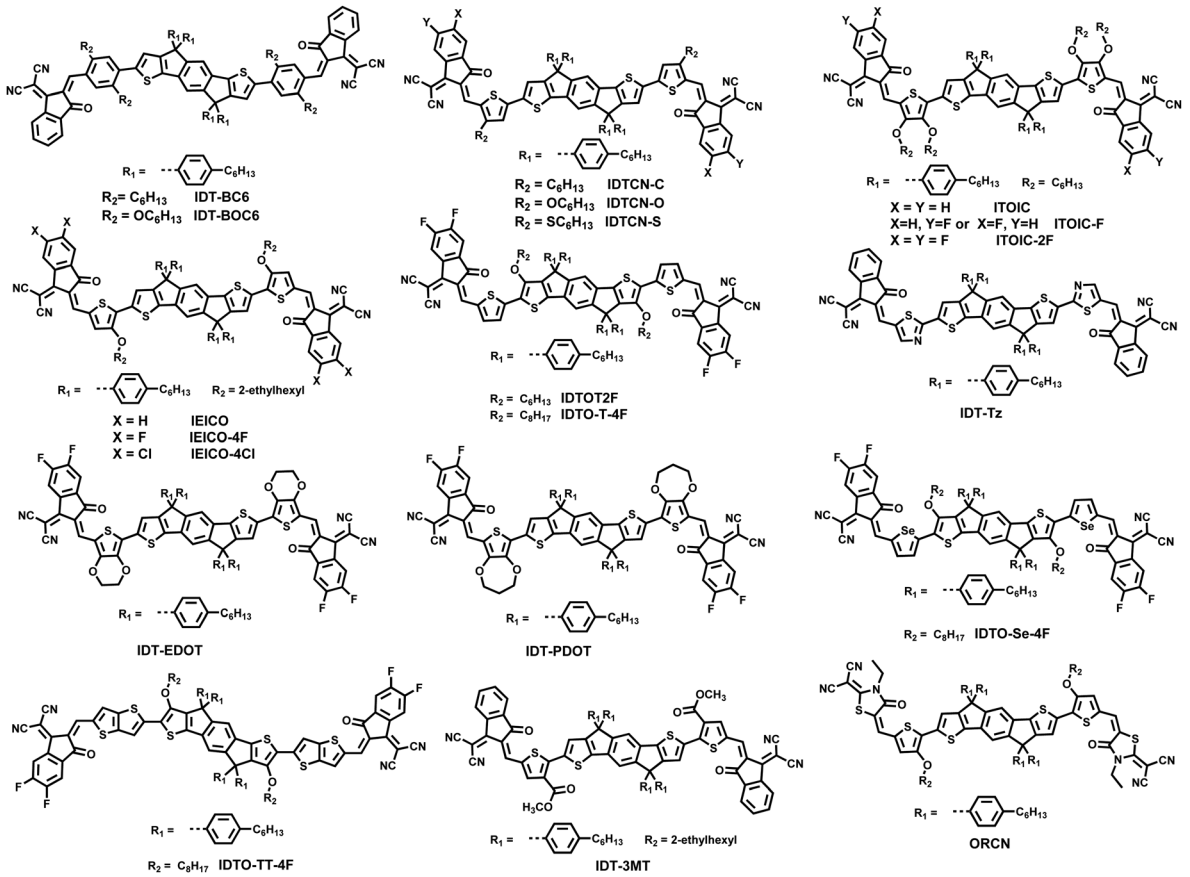

Fig. 12 Chemical structures of A–π–D–π–A type NFAs with IDT as the core unit.

synthesis for the fused-ring electron acceptors.[70,115] The as-synthesized acceptors display broad absorption ranging from 550 to 850 nm. Compared with the counterpart DC6-IC without INCIs, all acceptors present much higher fluorescence quantum yields (η_{FL}). Besides, the solubility of these NFAs can be adjusted by the lateral alkyl chains, and thus the film morphology can be well optimized. Encouragingly, as shown in Fig. 14, the photovoltaic devices realize relatively high EQE_{EL} and a very low non-radiative recombination energy loss of approximately 0.2 eV. Due to the distinct advantages of DOC2C6-2F, its devices with PBDB-T as the donor afford a high PCE of 13.24%. A slightly enlarged central core such as naphthalene is also tried as well and two isomers NOC6F-1 and NOC6F-2 with two alkyloxy chains located at the different positions (2,6- and 1,5-) of the naphthalene unit are designed and synthesized.[116] As shown in Fig. 15, these two NFAs exhibit quite different molecular geometries and a large distortion occurs in simplified NOC6F-2 according to DFT calculations, which is disadvantageous for electron delocalization and π–π stacking. Hence, the twisted NFA NOC6F-2 only gives a PCE of 6.74%, whereas a much higher PCE of 10.62% is achieved for NOC6F-1, ascribed to its

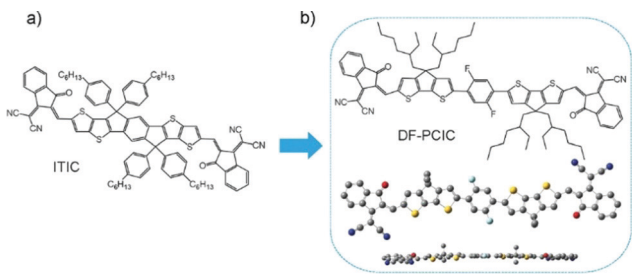

Fig. 13 (a) Chemical structure of ITIC. (b) Chemical structure and geometry of DF-PCIC. Copyright 2018, John Wiley & Sons.

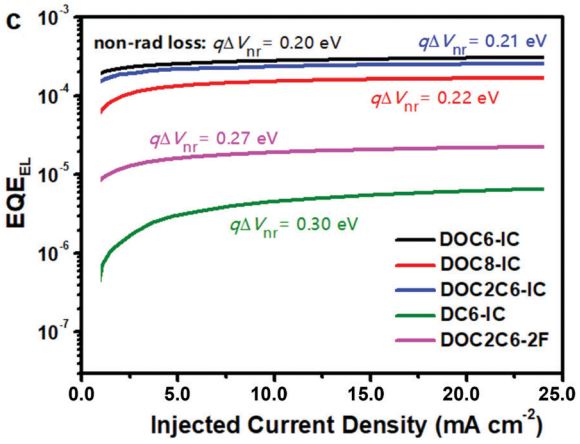

Fig. 14 EQE_{EL} of the solar cells based on different acceptors. Copyright 2019, Macmillan Publishers.

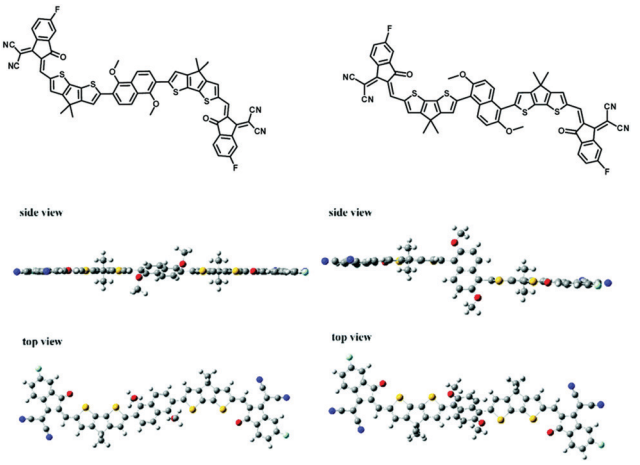

Fig. 15 Simulated molecular geometries obtained by DFT calculations for NOC6F-1 and NOC6F-2 in a simplified mode. Copyright 2018, Royal Society of Chemistry.

enhanced planarity and improved intermolecular π–π interactions (Fig. 15).

Similar to the INCI assisted CPs mentioned above, multiple noncovalent interactions could be introduced to the NFA molecular design *via* different combinations. Recently, 2-alkyloxy-5-fluorobenzene was also utilized as the central unit and a series of CPDT based acceptors (FOC6-IC, FOC6-FIC and FOC2C6-2FIC) were designed and synthesized.[117] As shown in Fig. 17 and 18, the single crystal results of FOC6-FIC and FOC2C6-2FIC confirm the existence of multiple INCIs, which play a critical role in forming the planar molecular backbones. Though all molecules possess very similar planar molecular configurations, the terminal constitutions would greatly influence the molecular stacking, orientation and crystallinity in the single crystals. Consequently, a high PCE of 12.36% is achieved for FOC2C6-2FIC-based devices, which is higher than that of FOC6-FIC (12.08%) and FOC6-IC (10.80%).

Except for the electron neutral and rich central unit, the electron deficient BT unit is adopted as the A_2 unit for the NFAs design and a series of A_1–D–A_2–D–A_1 type small molecular acceptors (BT-IC4F, BT2F-IC4F and BTOR-IC4F) have been

Table 2 Photovoltaic parameters of NFAs with the CPDT unit

NFAs	HOMO (eV)	LUMO (eV)	E_g (eV)	V_{oc} (V)	J_{sc} (mA/cm^2)	FF	PCE (%)	Ref.
DF-PCIC	−5.49	−3.77	1.59	0.91	15.66	0.72	10.14	114
DC6-IC	−5.53	−3.79	1.69	0.99	11.19	0.62	6.87	70
DOC6-IC	−5.33	−3.72	1.43	0.91	19.21	0.60	10.52	70
DOC8-IC	−5.36	−3.71	1.39	0.92	17.74	0.57	9.41	70
DOC2C6-IC	−5.38	−3.73	1.44	0.93	18.85	0.63	11.10	70
DOC2C6-2F	−5.49	−3.83	1.42	0.85	21.35	0.73	13.24	70
NOC6F-1	−5.55	−3.77	1.58	0.95	17.08	0.66	10.62	116
NOC6F-2	−5.50	−3.72	1.68	0.96	13.21	0.53	6.74	116
FOC6-IC	−5.42	−3.77	1.51	0.93	17.64	0.66	10.80	117
FOC6-FIC	−5.47	−3.81	1.47	0.89	19.18	0.71	12.08	117
FOC2C6-FIC	−5.51	−3.84	1.43	0.87	19.66	0.72	12.36	117
BT-IC4F	−5.89	−4.27	1.37	0.69	21.40	0.66	9.83	118
BT2F-IC4F	−5.98	−4.31	1.38	0.67	19.43	0.65	8.45	118
BTOR-IC4F	−5.92	−4.23	1.37	0.80	20.57	0.70	11.48	118
BDTS-4Cl	−5.45	−3.82	1.46	0.83	9.80	0.46	3.73	123
BDTC-4Cl	−5.35	−3.75	1.42	0.86	18.56	0.60	9.54	123
OF-PCIC	−5.66	−3.86	1.59	0.91	13.76	0.73	9.09	124
HFO-PCIC	−5.50	−3.81	1.48	0.93	12.62	0.71	8.36	124
DF-PCNC	−5.42	−3.81	1.54	0.86	18.16	0.73	11.63	125

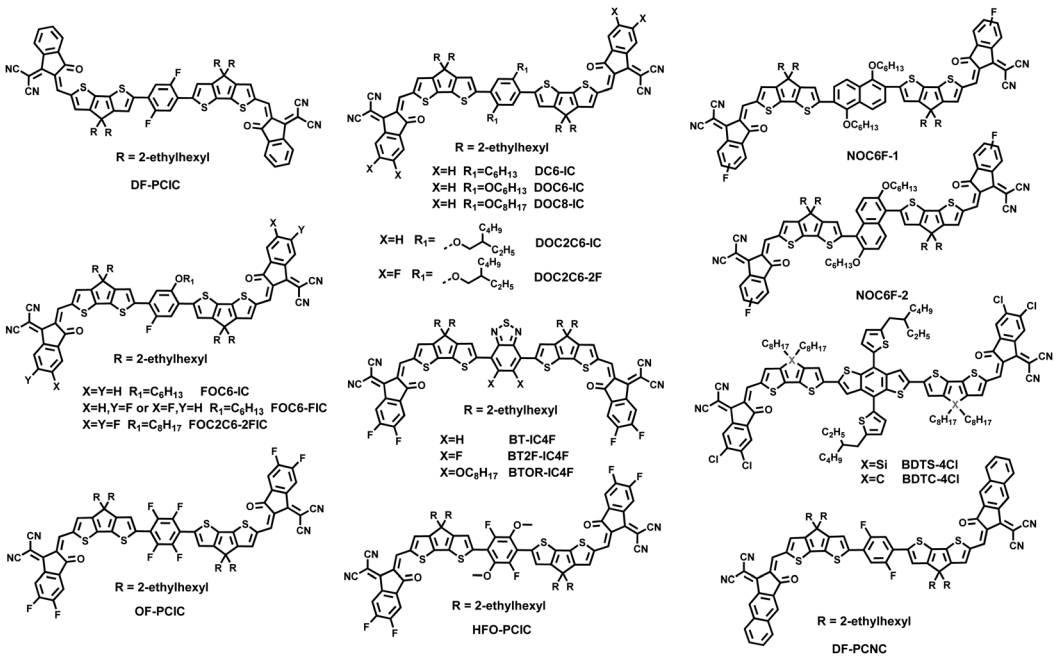

Fig. 16 Chemical structures of NFAs with the CPDT unit.

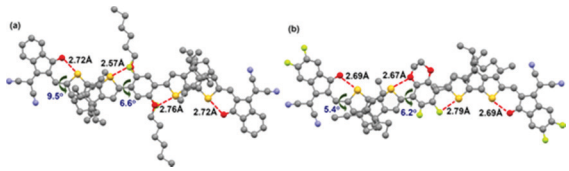

Fig. 17 Single crystal structures of (a) FOC6-IC and (b) FO2C6-2FIC. Copyright 2020, American Chemical Society.

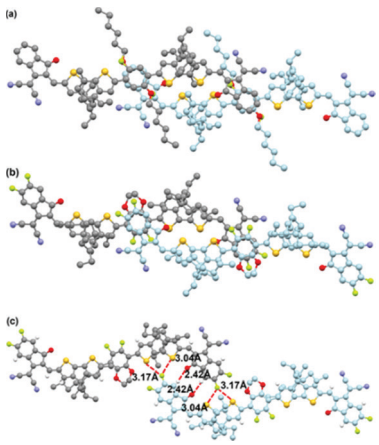

Fig. 18 Crystal stacking diagrams of (a) FOC6-IC dimer and (b and c) FOC2C6-2FIC dimer in the top view. Copyright 2020, American Chemical Society.

reported recently by several groups.[118–120] Due to the intramolecular S···N, F···S and O···S interactions, these acceptor molecules possess flat conformations for the molecular backbones. The introduction of two alkyloxy side chains at the BT unit could improve the solubility of small molecules and form appropriate blend film morphologies. Finally, devices based on BTOR-IC4F achieve a high PCE of 11.48%. Most importantly, PSCs based on BTOR-IC4F also exhibit the lowest non-radiative and radiative energy losses of 0.28 and 0.27 eV, respectively. Subsequently, acceptors with varied central units such as 3,4-difluorothiophene, benzodithiophene, *etc.*[121–125] have been developed, as shown in Fig. 16. The photovoltaic parameters of NFAs with CPDT units are also summarized in Table 2.

4. Conclusion and outlook

In conclusion, this review briefly introduces the design and construction of high performance photovoltaic materials including conjugated polymer donors, small molecular acceptors and hole transport polymers with the aid of INCIs. The introduction of INCIs can endow the polymer backbones with better planarity without significantly reducing their solubility. Thus, a good balance between processability and close packing for polymers can be achieved. The introduction of INCIs in the design and synthesis of nonfullerene acceptors can achieve a planar molecular backbone and bypass the complicated and low yield ring closure reactions, making it possible to acquire low-cost and high performance acceptor materials. The introduction of INCIs to conjugated polymers can endow the polymers with a ladder-like structure, allow the polymer chains to form closely packed structures, and make it possible for them to be used as hole transport materials for perovskite solar cells. Due to the solubility and dopant-free character, ladder-like conjugated polymers as hole transport materials for perovskite solar cells can greatly improve the device stability and durability. In all, we have demonstrated that INCIs are extremely useful in the design and synthesis of high performance optoelectronic materials.

For the outlook, the following aspects need to be explored:

(1) As for conjugated polymer donors, INCIs could elevate the planarity of the polymer backbones, which may bring solubility issues. Thus, balancing the molecular planarity and solubility is essential to guarantee the processability of materials. So, how to precisely and appropriately control the dynamic confinements of these polymers would be an effective way to achieve high performance materials.

(2) As for nonfullerene acceptors, the introduction of intramolecular noncovalent interactions could reduce the number of fused rings, thus simplifying the synthesis. Besides, low nonradiative energy loss is achieved in most photovoltaic devices based on these acceptors. However, the photovoltaic performance of nonfused acceptors is slightly lower than that of FREAs. It is highly important to further develop NFAs with the aid of INCIs. To obtain high performance acceptors, we should not only develop the noncovalent interaction type, but also consider the influence of intramolecular noncovalent interaction on the absorption, energy levels, solubility, *etc.*

(3) As for hole transport materials, the utilization of intramolecular noncovalent interaction in the design of conjugated polymers or small molecules is still rarely reported. Hence, the recognition to this field needs a few more examples. More importantly, our previous work already demonstrates its potential application in stable dopant-free perovskite solar cells.

In short, the introduction of INCIs can largely affect the molecular planarity, energy levels, absorption, *etc.* With the aid of INCIs, varied organic conjugated semiconductors are successfully developed and used in organic and perovskite solar cells. Empirical molecular design rules can greatly assist the reservation of the planar conformations, but morphology and device physics characterization should be involved in the future study so as to provide better understanding of the physical processes governing device performances. In addition, these INCI-based conjugated materials might also be utilized in other areas such as biological materials, photoelectric detectors, thermoelectric materials, *etc.*

Conflicts of interest

There are no conflicts to declare.

Acknowledgements

Financial support is acknowledged from the National Natural Science Foundation of China (51933001, 22075069 and U1704137).

Notes and references

1 Y.-J. Cheng, S.-H. Yang and C.-S. Hsu, *Chem. Rev.*, 2009, **109**, 5868–5923.
2 L. Lu, T. Zheng, Q. Wu, A. M. Schneider, D. Zhao and L. Yu, *Chem. Rev.*, 2015, **115**, 12666–12731.
3 Y. Li, *Acc. Chem. Res.*, 2012, **45**, 723–733.
4 C. B. Nielsen, S. Holliday, H.-Y. Chen, S. J. Cryer and I. McCulloch, *Acc. Chem. Res.*, 2015, **48**, 2803–2812.
5 J. Y. Kim, J.-W. Lee, H. S. Jung, H. Shin and N.-G. Park, *Chem. Rev.*, 2020, **120**, 7867–7918.
6 A. K. Jena, A. Kulkarni and T. Miyasaka, *Chem. Rev.*, 2019, **119**, 3036–3103.
7 M. Jung, S.-G. Ji, G. Kim and S. I. Seok, *Chem. Soc. Rev.*, 2019, **48**, 2011–2038.
8 J. Huang, Y. Yuan, Y. Shao and Y. Yan, *Nat. Rev. Mater.*, 2017, **2**, 17042.
9 C. J. Brabec, M. Heeney, I. McCulloch and J. Nelson, *Chem. Soc. Rev.*, 2011, **40**, 1185–1199.
10 W. Ni, X. Wan, M. Li, Y. Wang and Y. Chen, *Chem. Commun.*, 2015, **51**, 4936–4950.
11 M. C. Scharber and N. S. Sariciftci, *Prog. Polym. Sci.*, 2013, **38**, 1929–1940.
12 H. Yao, L. Ye, H. Zhang, S. Li, S. Zhang and J. Hou, *Chem. Rev.*, 2016, **116**, 7397–7457.
13 C. Yan, S. Barlow, Z. Wang, H. Yan, A. K. Y. Jen, S. R. Marder and X. Zhan, *Nat. Rev. Mater.*, 2018, **3**, 18003.
14 H. Sun, X. Guo and A. Facchetti, *Chem*, 2020, **6**, 1310–1326.
15 L. Ye, S. Zhang, L. Huo, M. Zhang and J. Hou, *Acc. Chem. Res.*, 2014, **47**, 1595–1603.
16 W. Li, K. H. Hendriks, M. M. Wienk and R. A. J. Janssen, *Acc. Chem. Res.*, 2016, **49**, 78–85.
17 Y. Liu, J. Zhao, Z. Li, C. Mu, W. Ma, H. Hu, K. Jiang, H. Lin, H. Ade and H. Yan, *Nat. Commun.*, 2014, **5**, 5293.
18 H. Hu, P. C. Y. Chow, G. Zhang, T. Ma, J. Liu, G. Yang and H. Yan, *Acc. Chem. Res.*, 2017, **50**, 2519–2528.
19 Y.-J. Cheng, M.-H. Liao, C.-Y. Chang, W.-S. Kao, C.-E. Wu and C.-S. Hsu, *Chem. Mater.*, 2011, **23**, 4056–4062.
20 D. Meng, H. Fu, C. Xiao, X. Meng, T. Winands, W. Ma, W. Wei, B. Fan, L. Huo, N. L. Doltsinis, Y. Li, Y. Sun and Z. Wang, *J. Am. Chem. Soc.*, 2016, **138**, 10184–10190.
21 D. Meng, D. Sun, C. Zhong, T. Liu, B. Fan, L. Huo, Y. Li, W. Jiang, H. Choi, T. Kim, J. Y. Kim, Y. Sun, Z. Wang and A. J. Heeger, *J. Am. Chem. Soc.*, 2016, **138**, 375–380.
22 Y. Cui, H. Yao, J. Zhang, K. Xian, T. Zhang, L. Hong, Y. Wang, Y. Xu, K. Ma, C. An, C. He, Z. Wei, F. Gao and J. Hou, *Adv. Mater.*, 2020, **32**, 1908205.
23 Q. Liu, Y. Jiang, K. Jin, J. Qin, J. Xu, W. Li, J. Xiong, J. Liu, Z. Xiao, K. Sun, S. Yang, X. Zhang and L. Ding, *Sci. Bull.*, 2020, **65**, 272–275.
24 Y. Lin and X. Zhan, *Mater. Horiz.*, 2014, **1**, 470–488.
25 P. Cheng and Y. Yang, *Acc. Chem. Res.*, 2020, **53**, 1218–1228.
26 Y.-N. Chen, M. Li, Y. Wang, J. Wang, M. Zhang, Y. Zhou, J. Yang, Y. Liu, F. Liu, Z. Tang, Q. Bao and Z. Bo, *Angew. Chem., Int. Ed.*, 2020, **59**, 22714–22720.
27 Y. Lin, Y. Firdaus, F. H. Isikgor, M. I. Nugraha, E. Yengel, G. T. Harrison, R. Hallani, A. El-Labban, H. Faber, C. Ma, X. Zheng, A. Subbiah, C. T. Howells, O. M. Bakr, I. McCulloch, S. D. Wolf, L. Tsetseris and T. D. Anthopoulos, *ACS Energy Lett.*, 2020, **5**, 2935–2944.
28 B. Fan, M. Li, D. Zhang, W. Zhong, L. Ying, Z. Zeng, K. An, Z. Huang, L. Shi, G. C. Bazan, F. Huang and Y. Cao, *ACS Energy Lett.*, 2020, **5**, 2087–2094.
29 L. Dou, Y. Liu, Z. Hong, L. Gang and Y. Yang, *Chem. Rev.*, 2015, **115**, 12633–12665.
30 Y. Chen, X. Wan and G. Long, *Acc. Chem. Res.*, 2013, **46**, 2645–2655.
31 J. Song and Z. Bo, *Sci. China: Chem.*, 2019, **62**, 9–13.
32 G. Zhang, J. Zhao, P. C. Y. Chow, K. Jiang, J. Zhang, Z. Zhu, J. Zhang, F. Huang and H. Yan, *Chem. Rev.*, 2018, **118**, 3447–3507.
33 S. Dey, *Small*, 2019, **15**, 1900134.
34 S. Li, C.-Z. Li, M. Shi and H. Chen, *ACS Energy Lett.*, 2020, **5**, 1554–1567.
35 Y. Huo, H.-L. Zhang and X. Zhan, *ACS Energy Lett.*, 2019, **4**, 1241–1250.
36 Z. H. Bakr, Q. Wali, A. Fakharuddin, L. Schmidt-Mende, T. M. Brown and R. Jose, *Nano Energy*, 2017, **34**, 271–305.
37 L. Calió, S. Kazim, M. Grätzel and S. Ahmad, *Angew. Chem., Int. Ed.*, 2016, **55**, 14522–14545.
38 L. R. Zhang, J. H. Wu, D. M. Li, W. H. Li, Q. B. Meng and Z. S. Bo, *J. Mater. Chem. A*, 2019, **7**, 14473–14477.
39 B. Yu, L. Zhang, J. Wu, K. Liu, H. Wu, J. Shi, Y. Luo, D. Li, Z. Bo and Q. Meng, *J. Mater. Chem. A*, 2020, **8**, 1417–1424.
40 K. Müller-Dethlefs and P. Hobza, *Chem. Rev.*, 2000, **100**, 143–168.
41 M. T. Rodgers and P. B. Armentrout, *Chem. Rev.*, 2016, **116**, 5642–5687.
42 A. S. Mahadevi and G. N. Sastry, *Chem. Rev.*, 2016, **116**, 2775–2825.
43 J. D. v. d. Waals, PhD dissertation, Unvertity of Leiden, 1873.
44 K. Liu, Y. Kang, Z. Wang and X. Zhang, *Adv. Mater.*, 2013, **25**, 5530–5548.
45 K. Müller-Dethlefs and P. Hobza, *Chem. Rev.*, 2000, **100**, 143–168.
46 J. Contreras-García, E. R. Johnson, S. Keinan, R. Chaudret, J.-P. Piquemal, D. N. Beratan and W. Yang, *J. Chem. Theory Comput.*, 2011, **7**, 625–632.
47 E. R. Johnson, S. Keinan, P. Mori-Sánchez, J. Contreras-García, A. J. Cohen and W. Yang, *J. Am. Chem. Soc.*, 2010, **132**, 6498–6506.
48 J. Starbuck, N. C. Norman and A. Guy Orpen, *New J. Chem.*, 1999, **23**, 969–972.
49 N. W. Alcock, in *Advances in Inorganic Chemistry and Radiochemistry*, ed. H. J. Emeléus and A. G. Sharpe, Academic Press, 1972, vol. 15, pp. 1–58.
50 H. Wang, W. Wang and W. J. Jin, *Chem. Rev.*, 2016, **116**, 5072–5104.
51 A. Bauzá, T. J. Mooibroek and A. Frontera, *ChemPhysChem*, 2015, **16**, 2496–2517.
52 P. Su, H. Chen and W. Wu, *Sci. China: Chem.*, 2016, **59**, 1025–1032.
53 L. C. Gilday, S. W. Robinson, T. A. Barendt, M. J. Langton, B. R. Mullaney and P. D. Beer, *Chem. Rev.*, 2015, **115**, 7118–7195.
54 M. Giese, M. Albrecht and K. Rissanen, *Chem. Rev.*, 2015, **115**, 8867–8895.
55 L. Yang, X. Tan, Z. Wang and X. Zhang, *Chem. Rev.*, 2015, **115**, 7196–7239.
56 R. J. Thibault, P. J. Hotchkiss, M. Gray and V. M. Rotello, *J. Am. Chem. Soc.*, 2003, **125**, 11249–11252.
57 Z. Wang, G. An, Y. Zhu, X. Liu, Y. Chen, H. Wu, Y. Wang, X. Shi and C. Mao, *Mater. Horiz.*, 2019, **6**, 733–742.
58 X. Ma and H. Tian, *Acc. Chem. Res.*, 2014, **47**, 1971–1981.
59 D. Bhowmick and G. Mugesh, *Org. Biomol. Chem.*, 2015, **13**, 10262–10272.
60 A. J. Mukherjee, S. S. Zade, H. B. Singh and R. B. Sunoj, *Chem. Rev.*, 2010, **110**, 4357–4416.
61 F. T. Burling and B. M. Goldstein, *J. Am. Chem. Soc.*, 1992, **114**, 2313–2320.
62 E. Jin, C. Du, M. Wang, W. Li, C. Li, H. Wei and Z. Bo, *Macromolecules*, 2012, **45**, 7843–7854.
63 H. Huang, Z. Chen, R. P. Ortiz, C. Newman, H. Usta, S. Lou, J. Youn, Y.-Y. Noh, K.-J. Baeg, L. X. Chen, A. Facchetti and T. Marks, *J. Am. Chem. Soc.*, 2012, **134**, 10966–10973.
64 R. Qin, W. Li, C. Li, C. Du, C. Veit, H.-F. Schleiermacher, M. Andersson, Z. Bo, Z. Liu, O. Inganäs, U. Wuerfel and F. Zhang, *J. Am. Chem. Soc.*, 2009, **131**, 14612–14613.
65 G. Li, X. Gong, J. Zhang, Y. Liu, S. Feng, C. Li and Z. Bo, *ACS Appl. Mater. Interfaces*, 2016, **8**, 3686–3692.
66 Q. Liu, C. Li, E. Jin, Z. Lu, Y. Chen, F. Li and Z. Bo, *ACS Appl. Mater. Interfaces*, 2014, **6**, 1601–1607.
67 P. Cheng, G. Li, X. Zhan and Y. Yang, *Nat. Photonics*, 2018, **12**, 131–142.
68 J. Hou, O. Inganäs, R. H. Friend and F. Gao, *Nat. Mater.*, 2018, **17**, 119–128.
69 Y. Liu, Z. Zhang, S. Feng, M. Li, L. Wu, R. Hou, X. Xu, X. Chen and Z. Bo, *J. Am. Chem. Soc.*, 2017, **139**, 3356–3359.
70 H. Huang, Q. X. Guo, S. Y. Feng, C. E. Zhang, Z. Z. Bi, W. Y. Xue, J. J. Yang, J. S. Song, C. H. Li, X. J. Xu, Z. Tang, W. Ma and Z. S. Bo, *Nat. Commun.*, 2019, **10**, 3038.
71 W. Lee, H. Choi, S. Hwang, J. Y. Kim and H. Y. Woo, *Chem. – Eur. J.*, 2012, **18**, 2551–2558.
72 T. Liu, L. Huo, S. Chandrabose, K. Chen, G. Han, F. Qi, X. Meng, D. Xie, W. Ma, Y. Yi, J. M. Hodgkiss, F. Liu, J. Wang, C. Yang and Y. Sun, *Adv. Mater.*, 2018, **30**, 1707353.

73 T. Xia, Y. Cai, H. Fu and Y. Sun, *Sci. China: Chem.*, 2019, **62**, 662–668.
74 Y. Ma, Q. Zheng, Z. Yin, D. Cai, S.-C. Chen and C. Tang, *Macromolecules*, 2013, **46**, 4813–4821.
75 J. Song, C. Du, C. Li and Z. Bo, *J. Polym. Sci., Part A: Polym. Chem.*, 2011, **49**, 4267–4274.
76 G. Li, C. Kang, X. Gong, J. Zhang, W. Li, C. Li, H. Dong, W. Hu and Z. Bo, *J. Mater. Chem. C*, 2014, **2**, 5116–5123.
77 G. Li, C. Kang, X. Gong, J. Zhang, C. Li, Y. Chen, H. Dong, W. Hu, F. Li and Z. Bo, *Macromolecules*, 2014, **47**, 4645–4652.
78 Y. Zhou, M. Li, Y. Guo, H. Lu, J. Song, Z. Bo and H. Wang, *ACS Appl. Mater. Interfaces*, 2016, **8**, 31348–31358.
79 M. Svensson, F. Zhang, S. C. Veenstra, W. J. H. Verhees, J. C. Hummelen, J. M. Kroon, O. Inganäs and M. R. Andersson, *Adv. Mater.*, 2003, **15**, 988–991.
80 R. Xia, W.-Y. Lai, P. A. Levermore, W. Huang and D. D. C. Bradley, *Adv. Funct. Mater.*, 2009, **19**, 2844–2850.
81 J. H. Cook, J. Santos, H. Li, H. A. Al-Attar, M. R. Bryce and A. P. Monkman, *J. Mater. Chem. C*, 2014, **2**, 5587–5592.
82 K. T. Kamtekar, A. P. Monkman and M. R. Bryce, *Adv. Mater.*, 2010, **22**, 572–582.
83 C. Du, C. Li, W. Li, X. Chen, Z. Bo, C. Veit, Z. Ma, U. Wuerfel, H. Zhu, W. Hu and F. Zhang, *Macromolecules*, 2011, **44**, 7617–7624.
84 G. Li, B. Zhao, C. Kang, Z. Lu, C. Li, H. Dong, W. Hu, H. Wu and Z. Bo, *ACS Appl. Mater. Interfaces*, 2015, **7**, 10710–10717.
85 X. Gong, G. Li, C. Li, J. Zhang and Z. Bo, *J. Mater. Chem. A*, 2015, **3**, 20195–20200.
86 Y. Lin, F. Zhao, Y. Wu, K. Chen, Y. Xia, G. Li, S. K. K. Prasad, J. Zhu, L. Huo, H. Bin, Z.-G. Zhang, X. Guo, M. Zhang, Y. Sun, F. Gao, Z. Wei, W. Ma, C. Wang, J. Hodgkiss, Z. Bo, O. Inganäs, Y. Li and X. Zhan, *Adv. Mater.*, 2017, **29**, 1604155.
87 C. Du, W. Li, Y. Duan, C. Li, H. Dong, J. Zhu, W. Hu and Z. Bo, *Polym. Chem.*, 2013, **4**, 2773–2782.
88 H. Wei, Y.-H. Chao, C. Kang, C. Li, H. Lu, X. Gong, H. Dong, W. Hu, C.-S. Hsu and Z. Bo, *Macromol. Rapid Commun.*, 2015, **36**, 84–89.
89 H. Zhou, Q. Chen, G. Li, S. Luo, T.-b. Song, H.-S. Duan, Z. Hong, J. You, Y. Liu and Y. Yang, *Science*, 2014, **345**, 542–546.
90 Q. Jiang, Y. Zhao, X. Zhang, X. Yang, Y. Chen, Z. Chu, Q. Ye, X. Li, Z. Yin and J. You, *Nat. Photonics*, 2019, **13**, 460–466.
91 T. Leijtens, G. E. Eperon, N. K. Noel, S. N. Habisreutinger, A. Petrozza and H. J. Snaith, *Adv. Energy Mater.*, 2015, **5**, 1500963.
92 G. Niu, X. Guo and L. Wang, *J. Mater. Chem. A*, 2015, **3**, 8970–8980.
93 J. You, L. Meng, T.-B. Song, T.-F. Guo, Y. Yang, W.-H. Chang, Z. Hong, H. Chen, H. Zhou, Q. Chen, Y. Liu, N. De Marco and Y. Yang, *Nat. Nanotechnol.*, 2016, **11**, 75–81.
94 Y. Lin, J. Wang, Z.-G. Zhang, H. Bai, Y. Li, D. Zhu and X. Zhan, *Adv. Mater.*, 2015, **27**, 1170–1174.
95 S. Holliday, R. S. Ashraf, A. Wadsworth, D. Baran, S. A. Yousaf, C. B. Nielsen, C.-H. Tan, S. D. Dimitrov, Z. Shang, N. Gasparini, M. Alamoudi, F. Laquai, C. J. Brabec, A. Salleo, J. R. Durrant and I. McCulloch, *Nat. Commun.*, 2016, **7**, 11585.
96 Y. Lin, Z.-G. Zhang, H. Bai, J. Wang, Y. Yao, Y. Li, D. Zhu and X. Zhan, *Energy Environ. Sci.*, 2015, **8**, 610–616.
97 J. Yuan, T. Huang, P. Cheng, Y. Zou, H. Zhang, J. L. Yang, S.-Y. Chang, Z. Zhang, W. Huang, R. Wang, D. Meng, F. Gao and Y. Yang, *Nat. Commun.*, 2019, **10**, 570.
98 J. Yuan, Y. Zhang, L. Zhou, G. Zhang, H.-L. Yip, T.-K. Lau, X. Lu, C. Zhu, H. Peng, P. A. Johnson, M. Leclerc, Y. Cao, J. Ulanski, Y. Li and Y. Zou, *Joule*, 2019, **3**, 1140–1151.
99 C. Zhu, J. Yuan, F. Cai, L. Meng, H. Zhang, H. Chen, J. Li, B. Qiu, H. Peng, S. Chen, Y. Hu, C. Yang, F. Gao, Y. Zou and Y. Li, *Energy Environ. Sci.*, 2020, **13**, 2459–2466.
100 X. Li, F. Pan, C. Sun, M. Zhang, Z. Wang, J. Du, J. Wang, M. Xiao, L. Xue, Z.-G. Zhang, C. Zhang, F. Liu and Y. Li, *Nat. Commun.*, 2019, **10**, 519.
101 Y. Liu, C. E. Zhang, D. Hao, Z. Zhang, L. Wu, M. Li, S. Feng, X. Xu, F. Liu, X. Chen and Z. Bo, *Chem. Mater.*, 2018, **30**, 4307–4312.
102 Y. Liu, M. Li, X. Zhou, Q. Jia, S. Feng, P. Jiang, X. Xu, W. Ma, H. Li and Z. Bo, *ACS Energy Lett.*, 2018, **3**, 1832–1839.
103 D. Liu, B. Kan, X. Ke, N. Zheng, Z. Xie, D. Lu and Y. Liu, *Adv. Energy Mater.*, 2018, **8**, 1801618.
104 Y. Liu, M. Li, J. Yang, W. Xue, S. Feng, J. Song, Z. Tang, W. Ma and Z. Bo, *Adv. Energy Mater.*, 2019, **9**, 1901280.
105 P. Jiang, S. Ming, Q. Jia, Y. Liu, H. Lu, M. Li, X. Xu, H. Li and Z. Bo, *J. Mater. Chem. A*, 2018, **6**, 21335–21340.
106 C. e. Zhang, P. Jiang, X. Zhou, S. Feng, Z. Bi, X. Xu, C. Li, Z. Tang, W. Ma and Z. Bo, *ACS Appl. Mater. Interfaces*, 2020, **12**, 40590–40598.
107 C. e. Zhang, P. Jiang, X. Zhou, H. Liu, Q. Guo, X. Xu, Y. Liu, Z. Tang, W. Ma and Z. Bo, *J. Mater. Chem. A*, 2020, **8**, 2123–2130.
108 S. Yu, Y. Chen, L. Yang, P. Ye, J. Wu, J. Yu, S. Zhang, Y. Gao and H. Huang, *J. Mater. Chem. A*, 2017, **5**, 21674–21678.
109 H. Yao, Y. Chen, Y. Qin, R. Yu, Y. Cui, B. Yang, S. Li, K. Zhang and J. Hou, *Adv. Mater.*, 2016, **28**, 8283–8287.
110 H. Yao, Y. Cui, R. Yu, B. Gao, H. Zhang and J. Hou, *Angew. Chem.*, 2017, **56**, 3045–3049.
111 Y. Cui, C. Yang, H. Yao, J. Zhu, Y. Wang, G. Jia, F. Gao and J. Hou, *Adv. Mater.*, 2017, **29**, 1703080.
112 S. Park, G. Park, S. Choi, Y. Kim, S. Park, C. Park, M. Cho and D. Choi, *J. Mater. Chem. C*, 2018, **6**, 7549–7556.
113 J. Wu, Y. Xu, Z. Yang, Y. Chen, X. Sui, L. Yang, P. Ye, T. Zhu, X. Wu, X. Liu, H. Cao, A. Peng and H. Huang, *Adv. Energy Mater.*, 2019, **9**, 1803012.
114 S. Li, L. Zhan, F. Liu, J. Ren, M. Shi, C.-Z. Li, T. P. Russell and H. Chen, *Adv. Mater.*, 2018, **30**, 1705208.
115 M. Chang, L. Meng, Y. Wang, X. Ke, Y. Yi, N. Zheng, Z. Xie, M. Zhang, Y. Yi, H. Zhang, X. Wan, C. Li and Y. Chen, *Chem. Mater.*, 2020, **32**, 2593–2604.
116 R. Zheng, Q. X. Guo, D. Hao, C. E. Zhang, W. Y. Xue, H. Huang, C. H. Li, W. Ma and Z. S. Bo, *J. Mater. Chem. C*, 2019, **7**, 15141–15147.
117 S. Feng, M. Li, N. Tang, X. Wang, H. Huang, G. Ran, Y. Liu, Z. Xie, W. Zhang and Z. Bo, *ACS Appl. Mater. Interfaces*, 2020, **12**, 4638–4648.
118 Y. Wang, Z. Liu, X. Cui, C. Wang, H. Lu, Y. Liu, Z. Fei, Z. Ma and Z. Bo, *J. Mater. Chem. A*, 2020, **8**, 12495–12501.
119 C. He, Y. Li, S. Li, Z.-P. Yu, Y. Li, X. Lu, M. Shi, C.-Z. Li and H. Chen, *ACS Appl. Mater. Interfaces*, 2020, **12**, 16700–16706.
120 S. Pang, X. Zhou, S. Zhang, H. Tang, S. Dhakal, X. Gu, C. Duan, F. Huang and Y. Cao, *ACS Appl. Mater. Interfaces*, 2020, **12**, 16531–16540.
121 R. Qin, W. Yang, S. Li, T.-K. Lau, Z. Yu, Z. Liu, M. Shi, X. Lu, C.-Z. Li and H. Chen, *Mater. Chem. Front.*, 2019, **3**, 513–519.
122 S. Li, L. Zhan, C. Sun, H. Zhu, G. Zhou, W. Yang, M. Shi, C.-Z. Li, J. Hou, Y. Li and H. Chen, *J. Am. Chem. Soc.*, 2019, **141**, 3073–3082.
123 Y.-Q.-Q. Yi, H. Feng, N. Zheng, X. Ke, B. Kan, M. Chang, Z. Xie, X. Wan, C. Li and Y. Chen, *Chem. Mater.*, 2019, **31**, 904–911.
124 S. Li, L. Zhan, W. Zhao, S. Zhang, B. Ali, Z. Fu, T.-K. Lau, X. Lu, M. Shi, C.-Z. Li, J. Hou and H. Chen, *J. Mater. Chem. A*, 2018, **6**, 12132–12141.
125 N. Wang, L. Zhan, S. Li, M. Shi, T.-K. Lau, X. Lu, R. Shikler, C.-Z. Li and H. Chen, *Mater. Chem. Front.*, 2018, **2**, 2006–2012.

